Computers & Geosciences ▮ (▮▮▮▮) ▮▮▮–▮▮▮

Contents lists available at ScienceDirect

Computers & Geosciences

journal homepage: www.elsevier.com/locate/cageo

Crusta: A new virtual globe for real-time visualization of sub-meter digital topography at planetary scales

Tony Bernardin [a,*], Eric Cowgill [b], Oliver Kreylos [b], Christopher Bowles [b], Peter Gold [b], Bernd Hamann [a], Louise Kellogg [b]

[a] Institute for Data Analysis and Visualization, Department of Computer Science, University of California, Davis, One Shields Avenue, Davis, CA 95616, USA
[b] Department of Geology, University of California, Davis, One Shields Avenue, Davis, CA 95616, USA

ARTICLE INFO

Article history:
Received 20 June 2009
Received in revised form
30 October 2009
Accepted 2 February 2010

Keywords:
Virtual globes
Terrain visualization
Digital elevation model
LiDAR

ABSTRACT

Virtual globes are becoming ubiquitous in the visualization of planetary bodies and Earth specifically. While many of the current virtual globes have proven to be quite useful for remote geologic investigation, they were never designed for the purpose of serving as virtual geologic instruments. Their shortcomings have become more obvious as earth scientists struggle to visualize recently released digital elevation models of very high spatial resolution (0.5–1 m^2/sample) and extent (>2000 km^2). We developed Crusta as an alternative virtual globe that allows users to easily visualize their custom imagery and more importantly their custom topography. Crusta represents the globe as a 30-sided polyhedron to avoid distortion of the display, in particular the singularities at the poles characteristic of other projections. This polyhedron defines 30 "base patches," each being a four-sided region that can be subdivided to an arbitrarily fine grid on the surface of the globe to accommodate input data of arbitrary resolution, from global (BlueMarble) to local (tripod LiDAR), all in the same visualization. We designed Crusta to be dynamic with the shading of the terrain surface computed on-the-fly when a user manipulates his point-of-view. In a similarly interactive fashion the globe's surface can be exaggerated vertically. The combination of the two effects greatly improves the perception of shape. A convenient pre-processing tool based on the GDAL library facilitates importing a number of data formats into the Crusta-specific multi-scale hierarchies that enable interactive visualization on a range of platforms from laptops to immersive geowalls and caves. The main scientific user community for Crusta is earth scientists, and their needs have been driving the development.

Published by Elsevier Ltd.

1. Introduction

A wide range of tectonic, geomorphic, ecologic, and anthropogenic processes dynamically shape the surface of the Earth. Thus, measuring topography and how it varies in space and time enables development and testing of quantitative models for these processes and understanding of the physics that underlies them and their temporal record. However, the range of length scales over which such processes operate is problematic because it means high-resolution (sub-meter) data spanning up to several 1000 km^2 are required. For example, offsets produced during a surface-rupture earthquake are typically centimeter- to meter-scale, but extend along a fault for tens to hundreds of kilometers.

LiDAR (Light Detection And Ranging) survey technology has provided an unprecedented increase in the accuracy and resolution of remotely acquired digital topographic data (Carter and Shrestha, 1997; Huising and Gomes-Pereira, 1998; Krabill et al., 1995; Ridgeway et al., 1997). As a result, LiDAR-derived digital elevation models (DEMs) and digital terrain models (DTMs) are being rapidly adopted across numerous disciplines in the geosciences. For example, LiDAR data have already been used in studies of active faulting (Cunningham et al., 2006; Engelkemeir and Khan, 2008; Gold et al., 2009; Haugerud et al., 2003; Hudnut et al., 2002; Johnson et al., 2004; Oskin et al., 2007), fault roughness and structural trend (Renard et al., 2006; Sagy et al., 2007; Wallace et al., 2006), geomorphic surface roughness and recovery over time (Filin, 2004; Frankel and Dolan, 2007; Smith et al., 2006; Staley et al., 2006; Wawrzyniec et al., 2007a, 2007b), active volcanoes and their associated hazards (Bohannon, 2007; Hofton et al., 2006; Mazzarini et al., 2007; Pesci et al., 2007; Ridgeway et al., 1997), the response of glaciers and ice sheets to a warming climate (Krabill et al., 1995; VanLooy et al., 2006), landslides (Glenn et al., 2006; McKeana and Roering, 2004; Van Den Eeckhaut et al., 2007), coastal geomorphology and the effects of hurricanes on shorelines (Carter and Shrestha, 1997; Irish and White, 1998; Robertson et al., 2007; Stockdon et al., 2007; Young

* Corresponding author.
E-mail address: tbernardin@ucdavis.edu (T. Bernardin).

0098-3004/$ - see front matter Published by Elsevier Ltd.
doi:10.1016/j.cageo.2010.02.006

and Ashford, 2006), and forest structure (Hopkinson et al., 2008; Lee and Lucas, 2007; Lim et al., 2003).

The widespread utility of LiDAR topographic data has led to a number of major efforts to gather large quantities of such data, including the southern California B4 Project[1] and GeoEarthScope surveys in southern and eastern California, the Intermountain Seismic Belt, and in northern California. These efforts have imaged the entire length of the San Andreas fault and of a number of associate faults (Prentice et al., 2009) within this complex plate boundary zone, and these data are now freely available at the OpenTopography Portal.[2] Likewise, the National Center for Airborne Laser Mapping (NCALM)[3] has surveyed sites for a diverse range of research projects supported by the National Science Foundation, the data for which are also freely available.[4] Individual states have also invested in airborne LiDAR scans to evaluate flood hazards due to hurricanes (North Carolina)[5] and levee breaks (California).[6]

Although LiDAR data are increasingly available, few tools exist that allow visualization and analysis of such high-resolution topography data over large spatial extents. While our previous topography visualization application, the Real-time Interactive Mapping System or RIMS (Bernardin et al., 2006), could already handle very large data, it was limited by a "flat-Earth" model that did not represent the curvature of the planet, and so is not appropriate in cases where a region of interest has such large spatial extents that distortions due to projection onto a flat map are not acceptable. Such is the case with the complete San Andreas fault data described above. Although existing virtual globe applications such as Google Earth resolve the problem of distortions in flat-earth representations, they suffer several other problems.

One problem with existing virtual globes is that it is either hard or impossible to import custom high-resolution topography data such as LiDAR DEMs. Google Earth, for example, uses a fixed global topography model. Although users can import hill-shaded images and drape them over the underlying model, or "patch" the model by converting their topographic data into three-dimensional (3D) objects, both have drawbacks. Specifically, hill-shaded imagery only appears correct when viewed from above, and is increasingly distorted either as the view zooms in or moves towards horizontal. More importantly, because the shading is precomputed from a fixed position, draped hill-shade images cannot provide shading changes in response to interactive movement of the 3D model, which provides strong shape cues that enable object recognition (Ramachandran, 1988). Likewise, importing topography as 3D objects is both cumbersome and only works for small data sets, because Google Earth's built-in multi-resolution rendering algorithm does not apply to imported 3D objects.

A second problem is that most existing virtual globe representations use a latitude–longitude grid as the basis for their topography models. This approach leads to significant distortion close to the poles due to the convergence of the longitude lines (Fig. 1). The Bing Maps[7] virtual globe hides this problem by masking the poles.

To address these problems we created a new virtual globe application, Crusta, following the same design principles as those we used to develop RIMS. As with RIMS, we have developed Crusta though a collaborative partnership between computer scientists (Bernardin, Kreylos, Hamann) and geoscientists (Cowgill, Bowles, Kellogg). Importantly, the geoscientists were intimately involved in the design and implementation process to ensure that Crusta is relevant to the needs of geoscience research. Crusta's aim is not to replace other virtual globes, which offer instant access to quality data and large amounts of contextual information, but rather to provide a specialized scientific instrument to enable the study of Earth-surface processes through visual analysis of large-extent, high-resolution topography and image data. Crusta does not stream fixed topography data from a central data warehouse, but instead assumes that users want to build data sets that are customized for their research needs and areas of investigation. In particular, Crusta allows users to create 3D terrain models of arbitrary resolution, and to visualize them without distortion due to map projection or biases introduced by hill-shading with a fixed illumination direction. As opposed to draped hill-shaded imagery, small terrain features are not only made visible by shading, but by proper geometric display. In other words, if a user were to visually extract a profile by introducing a cutting plane, the true profile would appear instead of the profile of the underlying lower-resolution terrain model. In general, the availability of a true 3D terrain model supports true scientific analysis, such as remote geologic mapping directly on 3D terrain models. The value of such tools has been demonstrated by recent studies in which RIMS was used to conduct remote geologic investigations (Raterman et al., 2007; Forte et al., 2010).

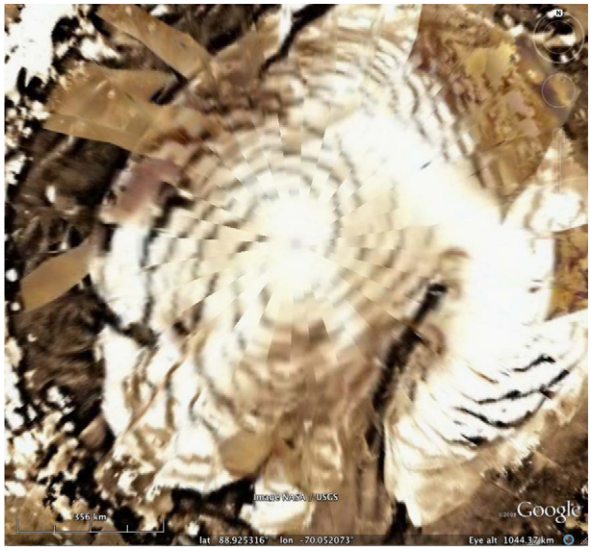

Fig. 1. Image of the north pole of Mars as viewed in Google Earth, demonstrating display distortion in polar regions. Such distortions occur in virtual globe representations employing a latitude–longitude grid as the basis for their topography models, motivating the use of 30-sided polyhedron in Crusta.

Crusta represents the globe as a 30-sided polyhedron to address the problem of distortion near the poles and to provide near-uniform and isotropic resolution everywhere on the sphere. The faces on this polyhedron are called "base patches" or "level-0" patches and are identical, four-sided spherical parallelograms, each of which is delineated by four great-circle segments. Each base patch can be subdivided into four level-1 patches, each of which can in turn be subdivided into four level-2 patches, and so forth. By successively subdividing base patches, Crusta can create arbitrarily fine curved grids, which in turn can represent topography or image data at arbitrarily fine resolutions, only limited by available external storage space. A pre-processing application based on the Geospatial Data Abstraction Library

[1] http://www.earthsciences.osu.edu/b4/Site/Welcome.html.
[2] http://www.OpenTopography.org/data.
[3] http://www.ncalm.org.
[4] http://calm.geo.berkeley.edu/ncalm/ddc.html.
[5] http://www.ncgs.state.nc.us/floodmap.html.
[6] http://www.water.ca.gov/levees/evaluation/lidar.cfm.
[7] http://www.bing.com/maps.

Please cite this article as: Bernardin, T., et al., Crusta: A new virtual globe for real-time visualization of sub-meter digital topography at planetary scales. Computers and Geosciences (2010), doi:10.1016/j.cageo.2010.02.006

(GDAL, 2009) is used to import topography or image data, and merge them into a new or existing Crusta database by adaptively subdividing existing patches until the resolution of the input data is matched. For example, it is possible to create a low-resolution background model using data with global coverage, such as NASA's next-generation Blue Marble, and then integrate very-high resolution data from a local LiDAR survey.

To visualize a pre-created database, Crusta uses a view-dependent, out-of-core rendering algorithm, which is a direct extension of that used in RIMS. This algorithm only loads and renders those parts of the database that are currently visible. As a result, Crusta can visualize data many times larger than the computer's main memory at interactive frame-rates (e.g., 50 frames/s). While Crusta's algorithm is different from the ones used by other virtual globe applications, it preserves the main advantage of such applications by providing seamless navigation of high-resolution topography at global scales, regardless of the performance of the computer's graphics subsystem.

Crusta is a prototype application, focusing on visualization of 3D terrain. However, Crusta's underlying data representation lends itself naturally to interaction with the terrain, and "human-in-the-loop" scientific analysis. As opposed to existing virtual globe applications, which are general-purpose tools for a broader user community, Crusta is streamlined for scientific uses. We are planning to develop mapping functionality very similar to what is available in RIMS, which has already been used to investigate deformation in the Kura fold-thrust belt in Azerbaijan (Forte et al., 2010) and the Karakoram fault in western China (Raterman et al., 2007), and to work with the community to determine what additional functionality is most useful for Earth science studies.

2. Design principles

As noted above, Crusta was designed and developed by a collaborative, interdisciplinary research team. While the geoscientists (Cowgill, Bowles, Kellogg) helped define the functionality required to achieve visual analysis of high resolution terrain data, the computer scientists (Bernardin, Kreylos, Hamann) devised highly efficient and robust algorithms needed to implement the design goals using highly intuitive user-interaction technology. Together we developed the software dynamically, with the geoscientists providing daily-to-weekly feedback as changes were made to the algorithm. This approach allowed rapid identification and resolution of shortcomings in algorithm design and implementation.

Our overarching goal for terrain visualization software is not to attempt to automate the process of virtual geologic investigation by means of algorithmic feature extraction. Rather, we follow a "human-in-the-loop" approach that relies upon human insight to define and identify features in high-resolution topographic data that are scientifically relevant for a particular investigation. Such an approach relies on the substantial specialist training of expert users for data interpretation. Thus, Crusta is merely an instrument facilitating the measurement and analysis process, much like a geologic compass, total station, or stereonet. As such, Crusta should be as specialized as required by geoscience researchers.

We developed the following specific design principles based on our past experiences with RIMS during both the development (Bernardin et al., 2006) and application phases (Raterman et al., 2007; Forte et al., 2010). For visualization purposes, Crusta must provide the highest dynamic range, to provide users with the maximum amount of access to their data, to allow them to perceive and work with the highest-resolution data available at the largest spatial extents possible. More specifically, Crusta must support the following:

1. Loading of standard GIS data from disk. Data availability should not be tied to specific providers.
2. Displaying data for any point on the globe and with arbitrary spatial extent. It should also be possible to merge several data sets of different resolutions, such as tripod LiDAR layered on airborne LiDAR layered on ASTER DEMs finally layered on SRTM DEMs.
3. Visualization of large data files while maintaining interactive display rates on a range of hardware platforms.
4. Exploitation of 3D visualization effects to best highlight surface topography.

These goals are implemented within the two components of Crusta that are discussed in the following sections: first a data pre-processor manages the creation and maintenance of an optimized, out-of-core, multi-scale data structure for visualization. The idea is to expend an expensive, one-time processing step in exchange for the ability to support many following interactive visualization sessions. Second, a viewer component produces the interactive display of the database by carefully choosing the appropriate multi-scale representation and applying dynamic shading and vertical exaggeration control.

3. Preparing high-resolution global data

The task of the pre-processing component of Crusta is to handle large terrain data and enable fast visualization. A key consideration is how to represent the two-dimensional input raster images (e.g., elevations in a DEM or colors in an air photo) on a globe. Most virtual globes map such data into a latitude–longitude parameterization of the surface. However, such a parameterization leads to distortions when mapping linear features from that space onto the sphere. This problem becomes especially visible close to the polar singularities (Fig. 1).

For Crusta we chose to use a base polyhedron, which is the approach used in whole-sphere models and finite element simulation methods such as HEALPix (Gorski et al., 2005) and CitcomS (Zhong et al, 2000; Tan et al., 2006). This approach reduces distortion by essentially distributing the two polar singularities over the multiple vertices of the polyhedral faces. The two most important constraints when choosing a base polyhedron to represent a height field over a sphere are *simplicity* and *uniformity* of subdivision. *Simplicity* is the main reason to choose a base polyhedron with only quadrilateral faces, such that a standard quadtree subdivision scheme can be used to refine each face to the desired resolution. Additionally, it is desirable to choose a base mesh with the least number of faces to reduce the number of special cases in the subdivision algorithm. *Uniformity*, on the other hand, favors base meshes that exhibit the highest similarity between any two quads in the subdivided mesh at any level. The (unattainable) ideal would be a base mesh where all quads at each subdivision level are identical.

The two primary choices for base meshes are the rhombic dodecahedron and rhombic triacontahedron, which have 12 and 30 identical rhombic faces, respectively. Both HEALPix and CitcomS employ a 12-sided polyhedron as a base mesh to approximate the sphere. In contrast, Crusta employs 30-sided rhombic triacontahedron. Although the rhombic dodecahedron is simpler, we use a rhombic triacontahedron because acute angles are 63.43° on its faces, meaning that each face and subdivided quad can be split into two almost equilateral triangles for rendering. In addition, the 30-sided polyhedron exhibits a higher

Please cite this article as: Bernardin, T., et al., Crusta: A new virtual globe for real-time visualization of sub-meter digital topography at planetary scales. Computers and Geosciences (2010), doi:10.1016/j.cageo.2010.02.006

degree of *uniformity*. For example, at subdivision level 8, the maximum discrepancies between any two quads in short diagonal length, long diagonal length, and aspect ratio are 18%, 7.5%, and 26%, respectively, whereas the same discrepancies for the rhombic dodecahedron are 43%, 24%, and 72%, respectively.

CitcomS was designed as a volumetric model for thermo-chemical convection. It extrudes layers of shells outward from the base patches. HEALPix, on the other hand, uses a principle closest to our approach in that it defines a hierarchy of grids on the globe surface. In contrast to Crusta's focus on visualization, HEALPix was developed for supporting simulations. As a result, the distribution and shape of the grid cells are carefully constrained to satisfy properties beneficial to those simulations such as preserving equal-area cells and the iso-latitude distribution of their centers. These constraints require that the most finely resolved level of the hierarchy be pre-generated through an optimization step. The hierarchy can be easily coarsened, but not refined without being recomputed in its entirety.

Keeping with the objective of flexibility and interactive performance of the representation, we chose a simpler approach based on the recursive subdivision of base patches. Fig. 2 illustrates how a base patch evolves through a quadtree refinement where a parent-patch splits into four child patches.

The patches are inscribed such that their vertices lie on the geoid and the mesh they form approximates the geoid. The subdivision proceeds in two phases: first, new vertices are computed as the linear mid-points between each pair of edge-vertices and the centroid. Second, the new points are projected back onto the geoid and connected into roughly quarter-sized patches as shown. The process is repeated for the newly produced children until the desired density of surface samples is reached.

Given fixed locations for the vertices of the base patches, the scheme produces refined sample locations deterministically. Thus, the sample positions need not be stored explicitly beyond those forming the base patches, reducing the Crusta database so that it contains only the raw data values: elevation relative to the geoid surface and the color. The deterministic nature of the scheme further facilitates merging/expanding and existing database with arbitrary new data.

Fig. 3 shows a comparison between the HEALPix "pixels" and our subdivided samples. Visualization performance is improved by batching the produced locations into grids of resolution n-by-n. (In the figure we have chosen $n=3$ for illustration purposes, but we typically use $n=65$, outlined with the magenta-colored line.)

Considering that the finest resolution can be arbitrarily chosen, we could simply refine the base polyhedron until even slightly distorted samples are dense enough to properly capture any and all detail from the input data. We note that subdivision does not necessarily occur uniformly across the polyhedron and refinement decisions can be made by local patch evaluation. In such a way we could accommodate non-uniformly sampled terrain data. Even so, we chose a polyhedron more closely approximating a sphere with the 30-sided rhombic Triacontahedron. We have found that the added base patches improve the behavior of the sample distribution and shape of the triangles of the mesh. An additional advantage of that polyhedron is that its faces are four-sided, which lend themselves to elegant and efficient quadtree approaches that are easily adapted to graphics hardware.

This subdivision scheme generates sample points that can be easily organized in a tiled hierarchy. The pre-processor generates a separate hierarchy for each base patch and records connectivity among patches. In order to populate the hierarchy from input data, the 3D Cartesian positions of the samples on the geoid are used to look up the corresponding elevation or color. We utilize the GDAL software library extensively to (a) process all the various file formats it supports and (b) process the projection from the Cartesian positions to geographic coordinates in the input's projective coordinate system and from there to pixels of the input rasters.

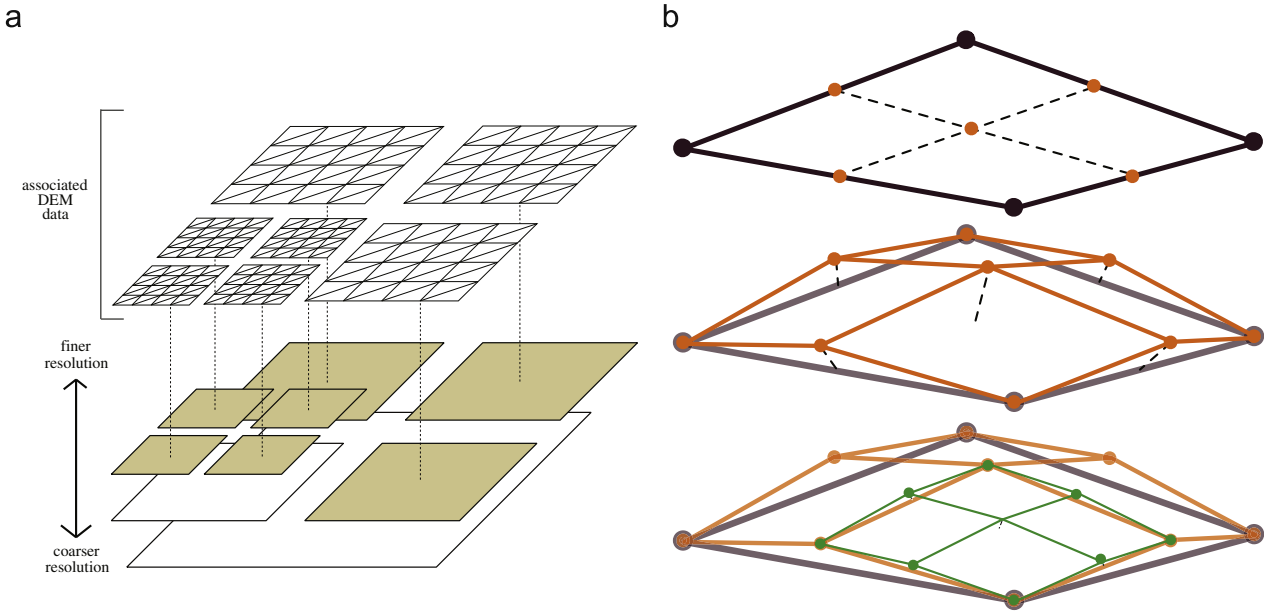

Fig. 2. Quadtree data representation implemented in Crusta: (a) Illustration of the general concept of a terrain quadtree, with a base patch at the bottom and children on top. The bottommost white box represents the whole scene at its coarsest resolution (the base patch). The colored boxes show the active tiles, which are those that are actually displayed on screen. For each active tile associated terrain data are also shown, although triangulated DEM meshes have been flattened to highlight the differences in geometry density with respect to area, rather than actual 3D positions (after Bernardin et al., 2006). Note this is a "flat-earth" representation. (b) Diagrams illustrating the spherical quadtree implementation in Crusta. At the top new vertices of level-1 child patches (in orange) are computed as linear mid-points of level-0 vertices (purple). These are then extruded to the surface of the sphere to form level-1 patches as illustrated by dashed lines in the middle sub-figure. The bottommost sub-figure shows one of the level-1 patches further subdivided and reprojected into four level-2 child patches (green). (For interpretation of the references to color in this figure legend, the reader is referred to the web version of this article.)

Please cite this article as: Bernardin, T., et al., Crusta: A new virtual globe for real-time visualization of sub-meter digital topography at planetary scales. Computers and Geosciences (2010), doi:10.1016/j.cageo.2010.02.006

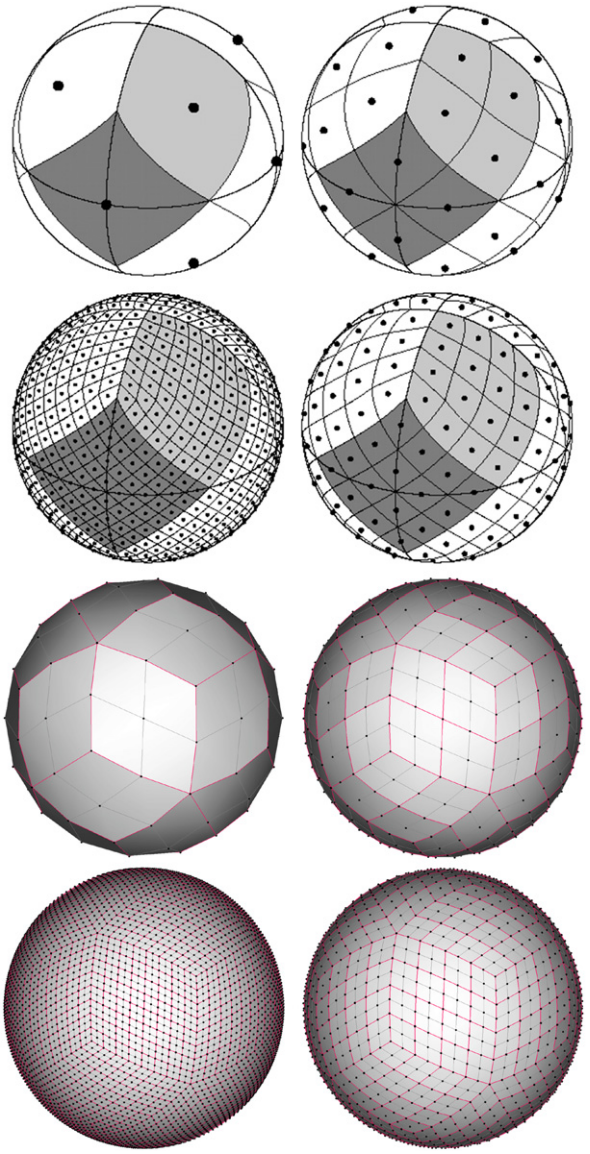

Fig. 3. Surface sample gridding as produced by HEALPix (top four spheres) and by Crusta (bottom four spheres).

The generation of the quadtrees is based on the following steps:

1. Generate the finest resolved levels of the hierarchy.
   1.1. Determine the coverage of the input data and its native resolution.
   1.2. Overlap each of the base tiles with the coverage. For each positive hit, produce child patches and continue the evaluation on those.
   1.3. Continue marching deeper through the tree until an overlapping refined patch is found that has adequate resolution in its $n \times n$ samples.
   1.4. Go through the samples of said patch, look up the value in the input raster, and store it in the hierarchy.
2. Generate the coarser resolved levels of the hierarchy.
   2.1. Start at the finest resolved patches for which data were fetched in the previous step.
   2.2. Move up one level and subsample from all the children to produce the data for the parents.
   2.3. Repeat 2.2 until the coarsest patch of all the hierarchies has had its data updated.

The process is similar if data are already processed into a hierarchy and new data need to be added. The difference being that instead of creating new patches to add to an empty hierarchy, an existing one is traversed and data appended unless the current refinement is not adequate. The advantage of this subdivision scheme is simplicity and global data coverage with low distortion. Thus, there is no need to consider projections beyond the pre-processing, which faithfully maps everything into a global 3D-space Crusta hierarchy. Elevations and color are kept in separate hierarchies and can be mixed and matched during visualization.

4. Visualizing a high-resolution globe

The pre-processed spatially tiled and multi-resolution representation of the input data provides an effective structure for facilitating visualization on a range of hardware platforms. Crusta takes advantage of this representation in a fashion similar to other current virtual globes. Specifically, the task of the visualization algorithm is to select the appropriate patches from the hierarchy to construct an approximated surface representation most appropriate for the current viewing parameters. A typical component of such level-of-detail selection approaches is the distance of the visualized data from the viewer: the greater the distance becomes the more small details become indistinguishable. At the limit, the pixel resolution of the display restricts how much information can be presented. In keeping to the idea of Crusta as a scientific instrument, we push the visualization to this limit. Fig. 4 shows a captured screen from Crusta displaying NASA's highest-resolution BlueMarble Next Generation data set in wire-frame mode. Even though the interior of meshes is not filled in this mode, the center of the display still seems to be a typical textured mesh.

Even higher-end graphics hardware might struggle with rendering the entire content of a high-definition display at such a mesh resolution. Our stance on the issue is that we are not interested in producing the most appealing image in the sense of an overview. Rather, we use a focus-and-context approach to delineate an area of interest, within which the most accurate representation of the data allowed by the display must be shown (one mesh vertex per pixel). Outside of this area we liberally decimate the mesh to liberate processing resources up to the point of preserving enough detail to provide appropriate context to the area in focus. The focus center remains fixed at the center of the screen, and as the user pans the terrain, patches that enter the focus area load in more detail while the ones exiting it discard detail. Likewise, detail is added and culled as the user zooms in and out of the terrain. As with other virtual globes, all these data transactions are cached, so that returning to a recently viewed location provides the data quasi-instantly.

One can best appreciate the visual display of Crusta through Videos 1 and 2. These videos illustrate Crusta visualization of the 2007 GeoEarthScope northern California airborne LiDAR data as merged with NASA's highest resolution BlueMarble NextGeneration dataset. As a visual instrument Crusta naturally benefits from advanced display hardware. We have designed Crusta to take advantage of the Vrui VR Toolkit (KeckCAVES, 2010) that enables it to run on a wide range of hardware, including laptops, workstations, immersive GeoWalls, and CAVES.

5. Comparison with existing virtual globes

Previously, it was not possible to visualize complete high-resolution LiDAR DEM data sets with currently available virtual

Please cite this article as: Bernardin, T., et al., Crusta: A new virtual globe for real-time visualization of sub-meter digital topography at planetary scales. Computers and Geosciences (2010), doi:10.1016/j.cageo.2010.02.006

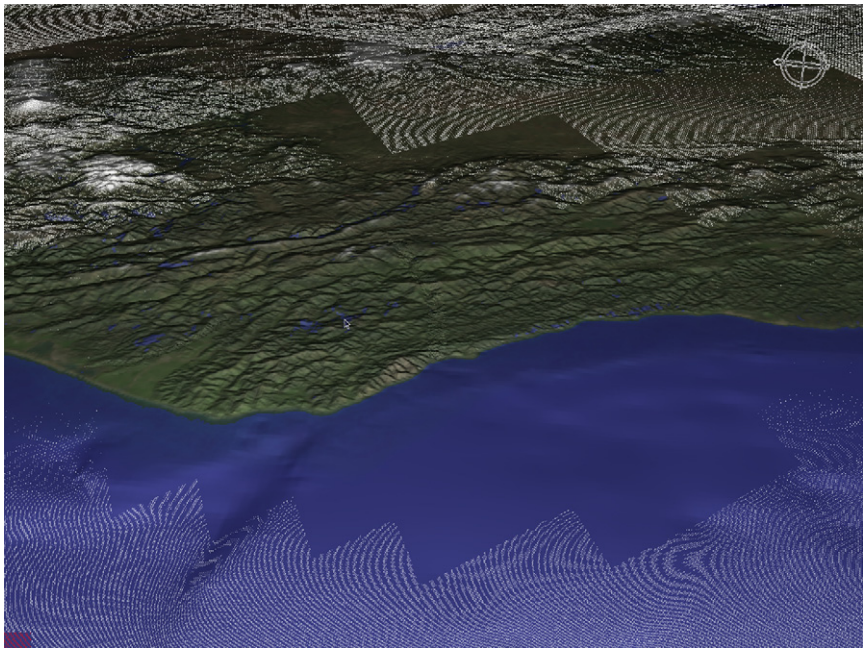

Fig. 4. Display of the terrain in Crusta using a wireframe rendering style. Mesh polygons are not filled, but instead only the edges are drawn. At the center of the screen, our level-of-detail chooses patches that cover one vertex per pixel, making it appear as if the mesh is filled. Thus, handling data at finer levels of details is not needed at this display resolution, allowing us to maximize display efficiency.

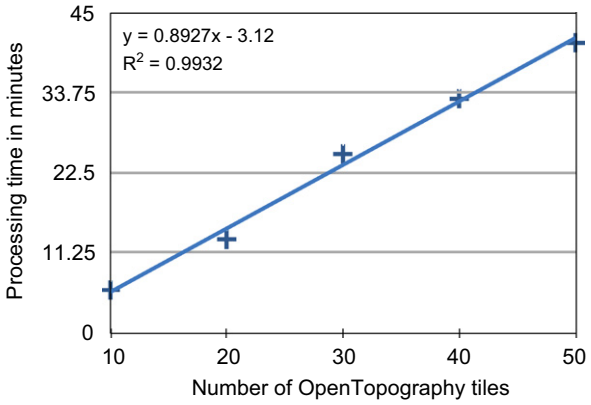

Fig. 5. Scale test performed on sets of 1 km^2 tiles with 0.5 m pixel resolution as served by the OpenTopograpy portal. The trend shows a linear increase in processing time with the number of tiles sourced.

globes or "flat-earth" terrain visualizers, a fact that directly motivated the development of Crusta. Here we provide a simple example of how Crusta can be used to reveal detailed features in the landscape of the sort that are of particular interest to neotectonic geologists because such details are essential for documenting active faulting and thus evaluating earthquake hazards. In particular, we use Crusta to examine the DEMs derived from the 2007 GeoEarthScope northern California airborne LiDAR surveys and served through the OpenTopography portal. The source data were pre-processed into a database and rendered in real time on a machine powered by a 2.6G Hz Intel Core i7 with 6 GB of main memory and an nVidia GeForce GTX 280 graphics card. The database was 410 GB on disk, demonstrating that Crusta can handle large data in real time. Furthermore, a quick scale test of the database processing performed on OpenTopography DEMs tiles shows a linear trend for the process (see Fig. 5). Images of the source data are also available as high-resolution hillshade images illuminated from 315° and 45°. These images can be draped over Google Earth. Thus, we also compare the visualization of such features in Crusta with their representation in the pre-processed hillshade images available in Google Earth. Although a complete case study such as those we've completed using RIMS (Raterman et al., 2007; Forte et al., 2010) is beyond the scope of the present work, this simple analysis helps to motivate the utility of the real-time visualization of high-resolution topography provided by Crusta.

Fig. 6 presents a portion of the new LiDAR data over Fort Ross, California. This image reveals an uphill-facing scarp that defines the active trace of the San Andreas fault in this area, and it is useful to note that it is on the basis of geomorphic details such as this scarp that neotectonic geologists identify and map active faults. In detail the figure provides a comparison of the pre-processed hillshade images draped over a lower-resolution digital elevation model in Google Earth (Fig. 6A and B) with the visualization of the true elevation data with a dynamic-lighting source provided by Crusta (Fig. 6C). As the figure demonstrates, it is considerably easier to locate and map the trace of the fault using the Crusta visualization. Besides the dominant scarp in the picture, it is also much easier to see subtle topographic features within Crusta for reasons. First, features are not hidden by shadows, as they are in static relief-shaded images. Second, the surface in Crusta is not a texture draped over lower-resolution topographic data as in Google Earth, but rather a dynamically illuminated surface that is created directly from the high-resolution topographic data.

Fig. 7 presents the same area and dataset as those shown in Fig. 6, except with a three-fold vertical exaggeration in both the cases. Because of the low-resolution of the underlying topographic data in the Google Earth visualization, the uphill-facing scarp becomes diffuse at this scale. In addition, the texture that is draped over the digital elevation model is stretched out, effectively ruining the visualization. By contrast, because Crusta uses the high-resolution digital elevation model, the scarp becomes a prominent feature when it is vertically exaggerated, allowing it to be more clearly distinguished.

Please cite this article as: Bernardin, T., et al., Crusta: A new virtual globe for real-time visualization of sub-meter digital topography at planetary scales. Computers and Geosciences (2010), doi:10.1016/j.cageo.2010.02.006

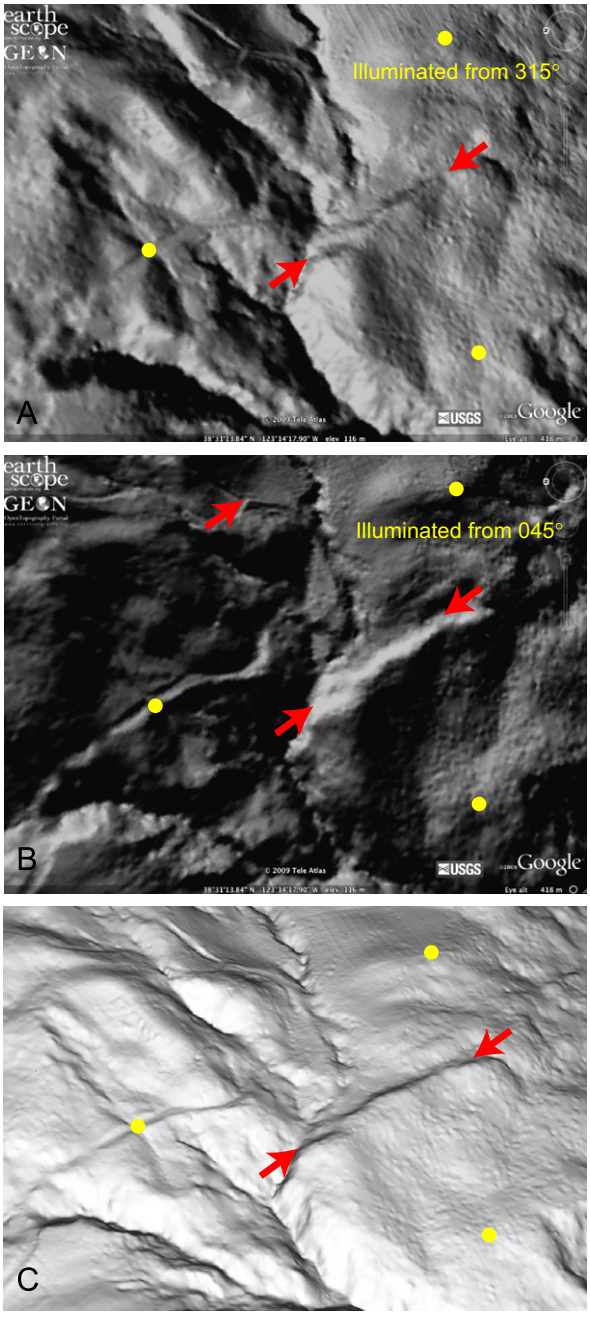

Fig. 6. Figures comparing Google Earth (A, B) and Crusta (C) visualizations of data from the 2007 GeoEarthScope northern California airborne LiDAR survey. All images show the same locality along the northern San Andreas fault, near Fort Ross, CA. Pairs of opposing red arrows point along an uphill facing scarp. Isolated red arrow indicates the location of a topographic detail (i.e., a drainage junction). Yellow dots are reference marks that are in the same three locations in all images to facilitate comparison. The scarp and drainage junction are much easier to distinguish using Crusta (C) than Google Earth hillshades (A, B). As such, Crusta provides an advantage to neotectonic geologists, because topographic details such as the scarp are the key criteria by which active deformation is identified. (For interpretation of the references to color in this figure legend, the reader is referred to the web version of this article.)

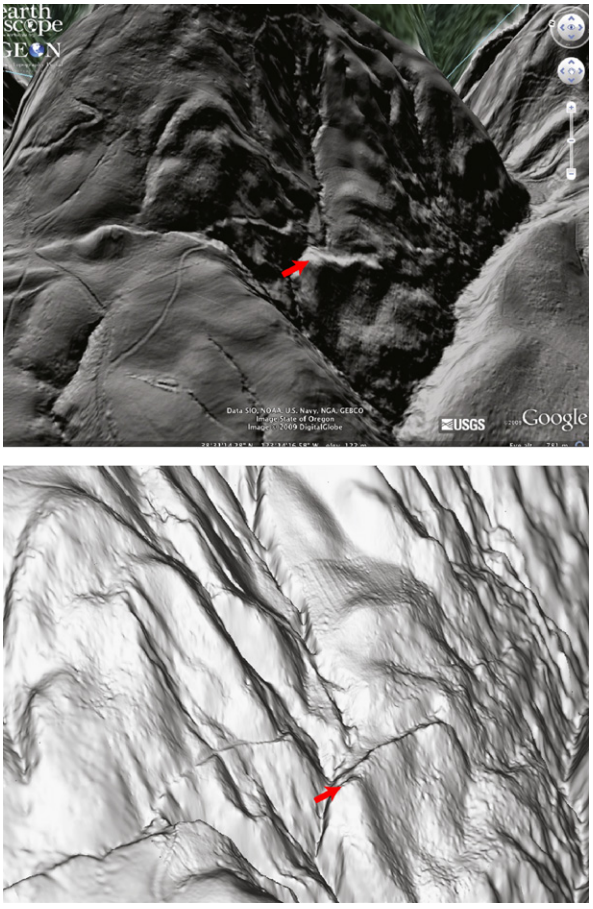

Fig. 7. Same as Fig. 6, but with vertical exaggeration. When exaggerating the vertical scale of the terrain, the Crusta display (bottom half) retains features properly due to the rendering of high-resolution topography. The Google Earth display (top half) drapes high-resolution imagery over coarse resolution topography, smearing the image of the scarp.

As a second preliminary test of Crusta's ability to facitilitate the discovery of detailed geologic features, we explored a small portion of 2008 LiDAR data flown over the fault systems in the Eastern California Shear Zone. In particular, we focused on the Owens Valley fault, an active, dominantly right-lateral fault with a component of oblique normal slip (Beanland and Clark, 1994). The last surface rupture event in the region occurred in 1872 and had an average lateral offset of 6 ± 2 m and normal offset of 1 ± 0.5 m (Beanland and Clark, 1994). Of interest is the contrast between the recorded geodetic rates of ~2 to ~7 mm/yr (Gan et al., 2000; McClusky et al., 2001; Dixon et al., 2003) and the geologically determined slip rates of ~1 to ~4 mm/yr (Beanland and Clark, 1994; Kirby et al., 2008; Lee et al., 2001; Bacon and Pezzopane, 2007). Finding new offset features and corresponding geologic slip rates on the Owens Valley fault may help explain the discrepancy between the geodetic and geologic slip rates.

We downloaded fifteen tiles from the OpenTopography data server that encompass an area of ~15 km^2 at a pixel resolution of 0.5 m. The data were processed into a 1.25 GB Crusta database in ~8 min. A graduate student geologist at UCDavis then used Crusta to search for features relevant to the study (i.e., scarps, offset streams, etc.). In a second step, the student used Google Earth with the KML of the LiDAR hillshade images to locate the same features extracted using Crusta before.

Although numerous matching spots were found, we restrict the discussion to two areas here. The first reveals a probable pressure ridge and deflected stream along the fault shown in Fig. 8a, b with 1 × vertical exaggeration in both Crusta and Google Earth. The feature is obvious in Crusta, but within Google Earth there are no recognizable features that suggest a pressure ridge besides the shadow outline. The prominent drainage that is easily distinguished in Fig. 8b is obscure and hard to recognize in Fig. 8a.

Please cite this article as: Bernardin, T., et al., Crusta: A new virtual globe for real-time visualization of sub-meter digital topography at planetary scales. Computers and Geosciences (2010), doi:10.1016/j.cageo.2010.02.006

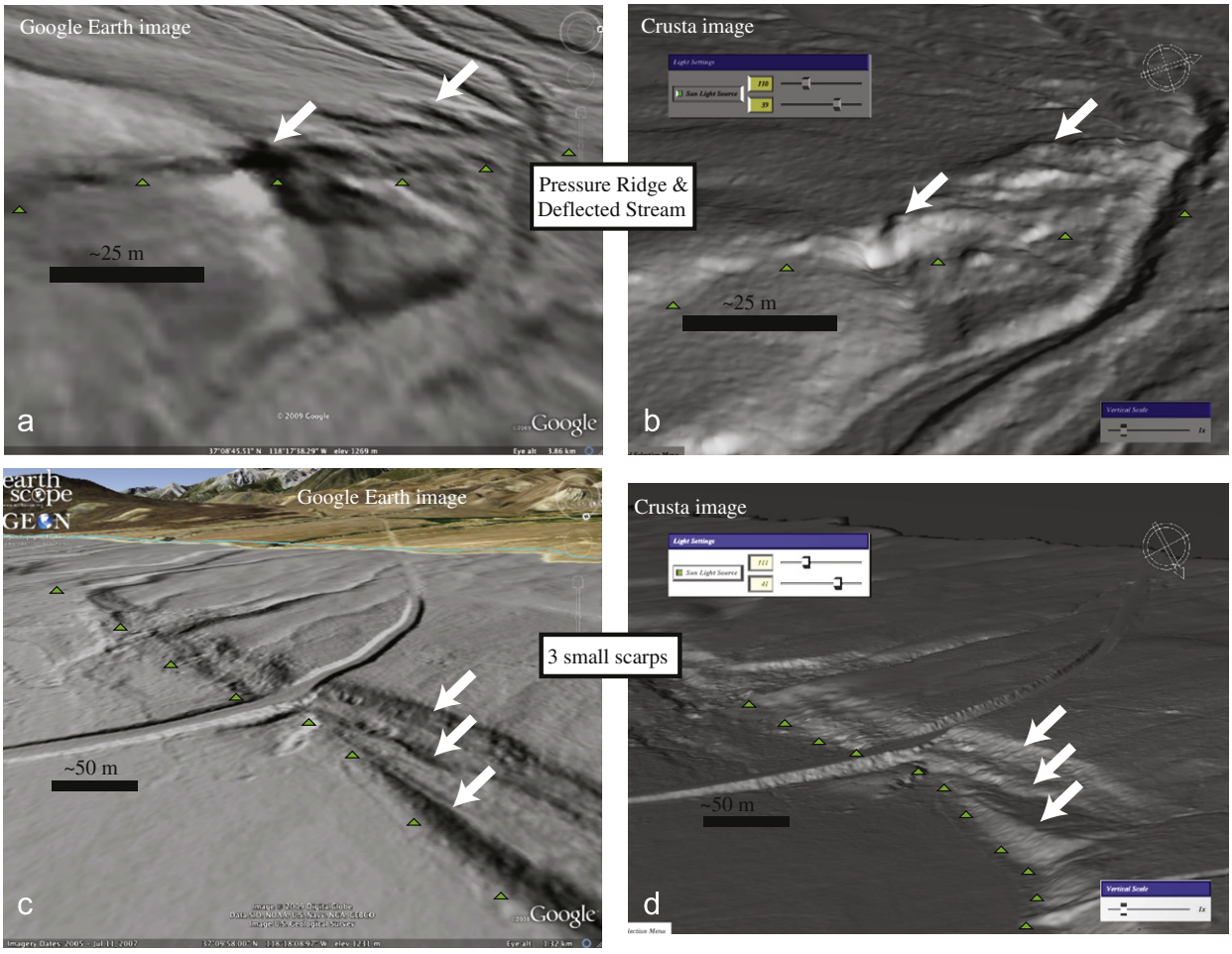

Fig. 8. For all figures, green arrow tips point to a fault trace. All scale bars are accurate only near their position on the image: (a) Google Earth image of probable pressure ridges (highlighted by white arrows). Note how the surface looks flat and only the shadows indicate possible topographic features. (b) Crusta image of same area as (a) with similar facing direction. The pressure ridges are very clear in the image (white arrows) and a drainage is easily distinguished. (c) Google Earth image of three small scarps (white arrows). No break in slope is obvious in the image. (d) Crusta image of same area as (c) with similar facing direction. Determining the edges and breaks in slope of the scarps (white arrows) is considerably easier in this image. All images use 2008 Eastern California Shear Zone LiDAR data from the OpenTopography portal. (For interpretation of the references to color in this figure legend, the reader is referred to the web version of this article.)

In the second area three small (<5 m) scarps record the normal movement of the fault shown in Fig. 8c, d. Again, the shadow outlines are the only distinguishing marks for these features in the Google Earth display (Fig. 8c); there are no clear breaks in slope. In comparison, the Crusta display (Fig. 8d) reveals obvious breaks in slope and scarps are easily identified.

The comparison illustrates how the dynamically shaded visualization using Crusta readily exposes such features critical in researching evidence of previous ruptures along the Owens Valley fault.

Smith and Clark (2005) discussed the advantages and disadvantages of various methods of visualizing digital elevation models. One important conclusion of their work was that the use of fixed-source, static relief-shaded imagery introduces non-negligible bias in the interpretation of the surface shape. Specifically, because a particular sun angle and azimuth must be specified to create a static hillshade from a digital elevation model, this approach will highlight certain features while simultaneously disguising or masking others that are covered by a shadow (see Fig. 5). Crusta avoids the problem of disguising topographic characteristics in static hillshades by using dynamic lighting to shade the digital elevation model. This approach allows a geoscientist to use lighting from any arbitrary direction and thus visualize topographic data without introducing bias from the illumination. Videos 1 and 2 highlight this effect.

In summary, a key strength of Crusta is its design to provide the maximum amount of topographic detail coupled with dynamic shading and exaggeration of the topography. In combination these effects considerably improve the perception of shape: as a user manipulates the point-of-view, the shading updates accordingly. In the same vein Crusta provides vertical exaggeration as do other virtual globes, but makes the process interactive. Thus, users obtain immediate and incremental visual feedback as they manipulate the exaggeration. The differing rates at which parts of the topography stretch or the accentuation of the shading provide yet another set of hints for the perception of shape.

6. Conclusions and future research directions

We have introduced Crusta, an alternative virtual globe that is well-suited to virtual geologic investigation of high-resolution (sub-meter) topography and color data on Earth. Crusta works in two steps: in the first, data of interest are pre-processed into an optimized, tiled and multi-scaled global representation. This is done by producing samples on the surface of the geoid through

Please cite this article as: Bernardin, T., et al., Crusta: A new virtual globe for real-time visualization of sub-meter digital topography at planetary scales. Computers and Geosciences (2010), doi:10.1016/j.cageo.2010.02.006

subdivision of a 30-sided base polyhedron and looking and storing the data values of the input at the sample locations. Our system makes extensive use of GDAL to facilitate data management. In the second step, the pre-processed data are fed to a real-time visualization component, which generates approximate surface representations by carefully choosing patches from the pre-processed hierarchy. We designed the approximation to provide the maximum level-of-detail the display hardware can resolve within a limited focal area, while maintaining lower-resolution representations beyond this area for context. To help illustrate Crusta's functionality, we have used it to visualize the 2007 GeoEarthScope northern California airborne LiDAR digital elevation model embedded in the most highly-resolved NASA Blue-Marble NextGeneration data sets. We expect Crusta to scale to even larger data sets given the multi-resolution approach that has been successful with other virtual globes. The strong point of the visualization is the faithful rendering of the topography coupled with dynamic shading and vertical exaggeration. Combined, these effects provide a greater perception of the shape of features on the Earth.

Future extensions of Crusta will be driven by the needs of the earth scientists using it as an instrument in "human-in-the-loop" analysis of high-resolution terrain data. Based on our work with RIMS and our current research needs, we plan to develop the following functions:

1. *Georeferenced line mapping*: This is the first function we plan to add to Crusta because it has proven to be a key feature in RIMS. This function will allow users to record observations by drawing georeferenced and attributed polylines directly on the virtual terrain model, while simultaneously interactively manipulating the terrain visualization in real time.
2. The *virtual geologic compass* (*VGC*) is another essential tool in RIMS for planned addition to Crusta. The VGC tool allows users to measure the 3D orientations of planes in space. The tool enables characterization of geologic structures such as folds by allowing geologists to use the line of intersection between a dipping sedimentary layer and topography to measure the orientations of the layer.
3. A *Profiler* tool for the generation of topographic profiles sampled along either a single line or across a swath. Both types of sampling are useful for quantifying landforms that record deformation, such as marine terraces that have been tilted due to folding or stream channels that have been displaced by repeated surface-rupturing earthquakes. With the profiler tool, the user will draw a box (of user-specified length, width, and orientation) that outlines a swath across the topography. The tool will then find all elevation data contained within the box, project them onto a profile line bisecting the box along its long axis, make a plot of elevation vs. profile distance along the bisector line, and then calculate mean, maximum, and minimum elevation within the swath as a function of profile position. Having the ability to export the sampled data will be important.
4. With a *displacement reconstruction* tool, the user will be able to interactively restore fault motion, returning deformed landforms to their original, unfaulted geometry. Specifically, the user will cut the terrain model along a given mapped fault line, and then interactively move one part of the model relative to the other. This tool would allow users to undo fault motion and thus test possible cross-fault correlations of landforms. Identifying multiple offset features along an active fault is important for measuring the history of fault slip (Gold, 2009).
5. *Fault editor* is a separate Vrui application for generating 3D fault models for input into Finite Element Model programs or earthquake simulations (Van Aalsburg et al., in press; Yıkılmaz et al., 2007). Merging Fault Editor and Crusta will provide a natural extension of the mapping function that has proven essential in RIMS. Specifically, using the line mapping tool described above, users can first map the surface traces of faults or edit existing fault maps imported from existing databases such as the Quaternary Fault and Fold Database of the United States.[8] Then, using the fault editor functionality, users can interactively extrapolate these surface traces into Earth's interior by fitting fault planes to subsurface distributions of earthquakes or other similar subsurface data.

Although we anticipate implementing these functions in Crusta ourselves, it should be straightforward for other users fluent in C++ to extend the code to incorporate additional functionality. Our ongoing experiences with other Vrui-based applications similar to Crusta and produced in our group serve as examples of such modification. For example, the code for Fault Editor (Van Aalsburg et al., in press) was written by Ph.D. students in Physics (Van Aalsberg) and Geology (Yikilmaz) by modifying a Vrui-based terrain viewer originally written by Kreylos. Likewise, computer scientists outside our group at the Desert Research Institute in Reno, NV, have used the Vrui VR development toolkit to develop several applications, mostly for scientific visualization. At Weill Cornell Medical College, scientists have similarly developed network visualization applications based on Vrui.

We expect to use Crusta for a number of ongoing and new geoscience research projects that are broadly centered on understanding active deformation and the temporal evolution of active fault slip. For example, we plan to use Crusta to investigate the geometry of active faulting within the Eastern California Shear Zone and the Intermountain Seismic Belt, with the goal of documenting fault-trace complexity produced over multiple earthquake ruptures. Another goal is to identify suites of landforms that are of a range of ages and thus show a range of total offsets. By using Crusta to document and reconstruct the displacements, and then using field-based studies to determine the ages of these landforms, we will be able to construct plots of displacement over time and thus determine the history of fault slip (Gold, 2009; Gold and Cowgill, 2009). Such histories are useful for determining how the rates at which faults change over time, which is important for understanding both the mechanics of earthquake faulting and quantifying earthquake hazards (e.g., Ben-Zion, 2008). Another potential research direction is to use Crusta in conjunction with regional mosaics of 30m/pixel DEMs derived from ASTER data to conduct remote, reconnaissance mapping of active faults and folds in seismically active but poorly documented regions such as NW Iraq, Iran, and eastern Turkey. Such work would build off of our previous work in the Greater Caucasus (Forte et al., 2010) and western Tibet (Raterman et al., 2007). Crusta is also a powerful tool for identifying features such as landslides in LiDAR data, and we anticipate it will be adopted by other groups for such studies as well.

For updates on the development and availability of Crusta, we refer the reader to the KeckCAVES website at http://keckcaves.ucdavis.edu.

Acknowledgements

Development of Crusta was supported by NASA Grant EOS/03-0663-0306 to Cowgill, by NSF Grant OCI-0753407 and by a gift from the W.M. Keck Foundation. We thank Peter Gold for

[8] http://earthquakes.usgs.gov/regional/qfaults.

performing the analysis of the Owens Valley fault. We also thank all members of the Visualization and Computer Graphics Research Group at the Institute for Data Analysis and Visualization (IDAV), Department of Computer Science, University of California, Davis.

Appendix A. Supplementary material

Supplementary data associated with this article can be found in the online version at doi:10.1016/j.cageo.2010.02.006.

References

Bacon, S.N., Pezzopane, S.K., 2007. A 25,000-year record of earthquakes on the Owens Valley fault near Lone Pine, California: implications for recurrence intervals, slip rates, and segmentation models. Geological Society of America Bulletin 119, 823–847.

Beanland, S., Clark, M.M., 1994. The Owens Valley fault zone, Eastern California, and surface faulting associated with the 1872 earthquake. US Geological Survey Bulletin 1982, 29.

Ben-Zion, Y., 2008. Collective behavior of earthquakes and faults: continuum-discrete transitions, progressive evolutionary changes, and different dynamic regimes. Reviews of Geophysics 46, RG4006, doi:10.1029/2008RG000260.

Bernardin, T., Cowgill, E., Gold, R., Hamann, B., Kreylos, O., Schmitt, A., 2006. Interactive mapping on 3-D terrain models. Geochemistry, Geophysics, Geosystems 7, Q10013, doi:10.1029/2006GC001335.

Bohannon, J., 2007. Stalking a volcanic torrent. Science 316, 1562–1563.

Carter, W.E., Shrestha, R.L., 1997. Airborne laser swath mapping: instant snapshots of our changing beaches. In: Proceedings of the Fourth International Conference: Remote Sensing for Marine and Coastal Environments, vol. I, Orlando, FL, Environmental Research Institute of Michigan, Ann Arbor, pp. 298 – 307.

Cunningham, D., Grebby, S., Tansey, K., Gosar, A., Kastelic, V., 2006. Application of airborne LiDAR to mapping seismogenic faults in forested mountainous terrain, southeastern Alps, Slovenia. Geophysical Research Letters 33, L20308, doi:10.1029/2006GL027014.

Dixon, T.H., Norabuena, E., Hotaling, L., 2003. Paleoseismology and global positioning system: earthquake-cycle effects and geodetic versus geologic fault slip rates in the eastern California shear zone. Geology 31, 55–58.

Engelkemeir, R.M., Khan, S.D., 2008. Lidar mapping of faults in Houston, Texas, USA. Geosphere 4, 172–182, doi:10.1130/GES00096.1.

Filin, S., 2004. Surface classification from airborne laser scanning data. Computers and Geosciences 30, 1033–1041.

Forte, A.M., Cowgill, E., Bernardin, T., Kreylos, O., Hamann, B., 2010. Late Cenozoic deformation of the Kura fold-thrust belt, southern Greater Caucasus. Geological Society of America Bulletin 122 (3/4), 465–486, doi:10.1130/B26464.1.

Frankel, K.L., Dolan, J.F., 2007. Characterizing arid region alluvial fan surface roughness with airborne laser swath mapping digital topographic data. Journal of Geophysical Research 112, F02025, doi:10.1029/2006JF000644.

Gan, W., Svarc, J.L., Savage, J.C., Prescott, W.H., 2000. Strain accumulation across the Eastern California shear zone at latitude 36°30′N. Journal of Geophysical Research 105, B7, 16, 229-16, 236.

GDAL Geospatial Data Abstraction Library. 〈http://www.gdal.org〉 (accessed on May 14, 2009).

Glenn, N.F., Streutker, D.R., Chadwick, D.J., Thackray, G.D., Dorsch, S.J., 2006. Analysis of LiDAR-derived topographic information for characterizing and differentiating landslide morphology and activity. Geomorphology 73, 131–148.

Gold, R.D., 2009. Latest Quaternary slip history of the central Altyn Tagh Fault, NW China, derived from faulted terrace risers. Ph.D. Dissertation, University of California, Davis, United States of America, 338 pp.

Gold, R.D., Cowgill, E., 2009. Derivation of "deep-time" fault-slip histories from dated and displaced landforms to test for secular variation in slip. Geological Society of America Abstracts with Programs 41 (7), 184.

Gold, R.D., Cowgill, E., Arrowsmith, J.R., Gosse, J., Chen, X., Wang, W.F., 2009. Riser diachroneity, lateral erosion, and uncertainty in rates of strike-slip faulting: a case study from Tuzidun along the Altyn Tagh Fault, NW China. Journal of Geophysical Research 114, B04401, doi:10.1029/2008JB005913.

Gorski, K.M., Hivon, E., Banday, A.J., Wandelt, B.D., Hansen, F.K., Reinecke, M., Bartelmann, M., 2005. HEALPix: a framework for high-resolution discretization and fast analysis of data distributed on the sphere. Astrophysical Journal 622, 759–771.

Haugerud, R.A., Harding, D.J., Johnson, S.Y., Harless, J.L., Weaver, C.S., Sherrod, B.L., 2003. High-resolution LiDAR topography of the Puget lowland, Washington: a bonanza for earth science. Geological Society of America Today 13, 4–10.

Hofton, M.A., Malavassi, E., Blair, J.B., 2006. Quantifying recent pyroclastic and lava flows at Arenal Volcano, Costa Rica, using medium-footprint LiDAR. Geophysical Research Letters, 33, doi:10.1029/2006GL027822.

Hopkinson, C., Chasmer, L., Hall, R.J., 2008. The uncertainty in conifer plantation growth prediction from multi-temporal LiDAR datasets. Remote Sensing of Environment 112, 1168–1180.

Hudnut, K.W., Borsa, A., Glennie, C., Minster, J.B., 2002. High-resolution topography along surface rupture of the 16 October 1999 Hector mine, California, earthquake (Mw 7.1) from airborne laser swath mapping. Bulletin of the Seismological Society of America 92, 1570–1576.

Huising, E.J., Gomes-Pereira, L.M., 1998. Errors and accuracy estimates of laser data acquired by various laser scanning systems for topographic applications. ISPRS Journal of Photogrammetry and Remote Sensing 53, 245–261.

Irish, J.L., White, T.E., 1998. Coastal engineering applications of high-resolution lidar bathymetry. Coastal Engineering 35, 47–71.

Johnson, S.Y., Nelson, A.R., Personius, S.F., Wells, R.E., Kelsey, H.M., Sherrod, B.L., Okumura, K., Koehler III, R., Witter, R.C., Bradley, L.A., Harding, D.J., 2004. Evidence for late Holocene earthquakes on the Utsalady Point fault, northern Puget Lowland, Washington. Bulletin of the Seismological Society of America 94, 2299–2316.

KeckCAVES Vrui VR Toolkit description. 〈http://www.keckcaves.org/software/vrui/index.html〉 (accessed May 14, 2010).

Kirby, E., Anandakrishnan, S., Phillips, F., Marrero, S., 2008. Late Pleistocene slip rate along the Owens Valley fault, eastern California. Geophysical Research Letters 35, L01304, doi:10.1029/2007GL031970.

Krabill, W.B., Thomas, R.H., Martin, C.F., Swift, R.N., Frederick, E.B., 1995. Accuracy of airborne laser altimetry of the Greenland ice sheet. International Journal of Remote Sensing 16, 1211–1222.

Lee, A.C., Lucas, R.M., 2007. A LiDAR-derived canopy density model for tree stem and crown mapping in Australian forests. Remote Sensing of Environment 111, 493–518.

Lee, J., Spencer, J., Owen, L., 2001. Holocene slip rate along the Owens Valley fault, California: implications for the recent evolution of the Eastern California Shear Zone. Geology 29 (9), 819–822.

Lim, K., Treitz, P., Wulder, M., St-Onge, B., Flood, M., 2003. LiDAR remote sensing of forest structure. Progress in Physical Geography 27 (1), 88–106.

Mazzarini, F., Pareschi, M.T., Favalli, M., Isola, I., Tarquini, S., Boschi, E., 2007. Lava flow identification and aging by means of lidar intensity: Mount Etna case. Journal of Geophysical Research, 112, doi:10.1029/2005JB004166.

McClusky, S.C., Bjornstad, S.C., Hager, B.H., King, R.W., Meade, B.J., Miller, M.M., Monastero, F.C., Souter, B.J., 2001. Present day kinematics of the eastern California shear zone from a geodetically constrained block model 28, 3369–3372Geophysical Research Letters 28, 3369–3372.

McKeana, J., Roering, J., 2004. Objective landslide detection and surface morphology mapping using high-resolution airborne laser altimetry. Geomorphology 57, 331–351.

Oskin, M., Le, K., Strane, M.D., 2007. Quantifying fault-zone activity in arid environments with high-resolution topography. Geophysical Research Letters, 34, doi:10.1029/2007GL031295.

Pesci, A., Fabris, M., Conforti, D., Loddo, F., Baldi, P., Anzidei, M., 2007. Integration of ground-based laser scanner and aerial digital photogrammetry for topographic modelling of Vesuvio volcano. Journal of Volcanology and Geothermal Research 162, 123–138.

Prentice, C.S., Crosby, C.J., Whitehill, C.S., Arrowsmith, J.R., Furlong, K.P., Phillips, D.A., 2009. Illuminating Northern California's Active Faults. Eos 90 (7), 55.

Ramachandran, V.S., 1988. Perceiving shape from shading. Scientific American 259, 76–83.

Raterman, N.S., Cowgill, E., Ding, L., 2007. Variable structural style along the Karakoram fault explained using triple-junction analysis of intersecting faults. Geosphere 3 (2), 71–85, doi:10.1130/GES00067.1.

Renard, F., Voisin, C., Marsan, D., Schmittbuhl, J., 2006. High resolution 3D laser scanner measurements of a strike-slip fault quantify its morphological anisotropy at all scales. Geophysical Research Letters 33, doi:10.1029/2005GL025038.

Ridgeway, J.R., Minster, J.B., Williams, N., Bufton, J.L., Krabill, W.B., 1997. Airborne laser altimetry survey of Long Valley, California. Geophysical Journal International 131, 267–280.

Robertson, V.W., Zhang, K., Whitman, D., 2007. Hurricane-induced beach change derived from airborne laser measurements near Panama City, Florida. Marine Geology 237, 191–205.

Sagy, A., Brodsky, E.E., Axen, G.J., 2007. Evolution of fault-surface roughness with slip. Geology 35, 283–286, doi:10.1130/G23235A.1.

Smith, M.J., Clark, C.D., 2005. Methods for the visualization of digital elevation models for landform mapping. Earth Surface Processes and Landforms 30, 885–900, doi:10.1002/esp.1210.

Smith, L.C., Sheng, Y., Magilligan, F.J., Smith, N.D., Gomez, B., Mertes, L.A.K., Krabill, W.B., Garvin, J.B., 2006. Geomorphic impact and rapid subsequent recovery from the 1996 Skeiðarársandur jökulhlaup, Iceland, measured with multi-year airborne LiDAR. Geomorphology 75, 65–75.

Staley, D.M., Wasklewicz, T.A., Blaszczynski, J.S., 2006. Surficial patterns of debris flow deposition on alluvial fans in Death Valley, CA using airborne laser swath mapping data. Geomorphology 74, 152–163.

Stockdon, H.F., Sallenger Jr., A.H., Holman, R.A., Howd, P.A., 2007. A simple model for the spatially-variable coastal response to hurricanes. Marine Geology 238, 1–20.

Tan, E., Choi, E., Thoutireddy, P., Gurnis, M., Aivazis, M., 2006. GeoFramework: coupling multiple models of mantle convection within a computational framework. Geochemistry, Geophysics, and Geosystems 7, Q06001, doi:10.1029/2005GC001155.

Please cite this article as: Bernardin, T., et al., Crusta: A new virtual globe for real-time visualization of sub-meter digital topography at planetary scales. Computers and Geosciences (2010), doi:10.1016/j.cageo.2010.02.006

Van Aalsburg, J., Yikilmaz, M.B., Kreylos, O., Kellogg, L.H., Rundle, J.B., 2009, Interactive editing of digital fault models. Concurrency and Computation: Practice and Experience. 10.1002/cpe.1525.

Van Den Eeckhaut, M., Poesen, J., Verstraeten, G., Vanacker, V., Nyssen, J., Moeyersons, J., van Beek, L.P.H., Vandekerckhove, L., 2007. Use of LiDAR-derived images for mapping old landslides under forest. Earth Surface Processes and Landforms 32, 754–769.

VanLooy, J., Forster, R., Ford, A., 2006. Accelerating thinning of Kenai Peninsula glaciers, Alaska. Geophysical Research Letters 33 (21), L21307, doi:10.1029/2006GL028060.

Wallace, J., Morris, B., Howarth, P., 2006. Identifying structural trend with fractal dimension and topography. Geology 34, 901–904, doi:10.1130/G22632A.1.

Wawrzyniec, T.F., Jones, R.R., McCaffrey, K., Imber, J., Holliman, N., Holdsworth, R.E., 2007a. Introduction: unlocking 3D earth systems-harnessing new digital technologies to revolutionize multi-scale geological models. Geosphere 3, 406–407.

Wawrzyniec, T.F., McFadden, L.D., Ellwein, A., Meyer, G., Scuderi, L., McAuliffe, J., Fawcett, P., 2007b. Chronotopographic analysis directly from point-cloud data: a method for detecting small, seasonal hillslope change, Black Mesa Escarpment, NE Arizona. Geosphere 3, 550–567.

Yıkılmaz, M.B., Van Aalsburg, J., Kreylos, O., Kellogg, L.H., Rundle, J.B., 2007. A 3D immersive fault visualizer and editor. EOS Transactions, American Geophysical Union 88 (52) Fall Meet. Suppl., Abstract IN13A-0904.

Young, A.P., Ashford, S.A., 2006. Application of airborne LiDAR for seacliff volumetric change and beach-sediment budget contributions. Journal of Coastal Research 22, 307–318.

Zhong, S., Zuber, M.T., Moresi, L.N., Gurnis, M., 2000. The role of temperature-dependent viscosity and surface plates in spherical shell models of mantle convection. Journal of Geophysical Research 105, 11063–11082.

Please cite this article as: Bernardin, T., et al., Crusta: A new virtual globe for real-time visualization of sub-meter digital topography at planetary scales. Computers and Geosciences (2010), doi:10.1016/j.cageo.2010.02.006